

# The Grating Imager System

BGGN 266 / PHYS 173  
Modern Physics Laboratory: Biological through Quantum Physics

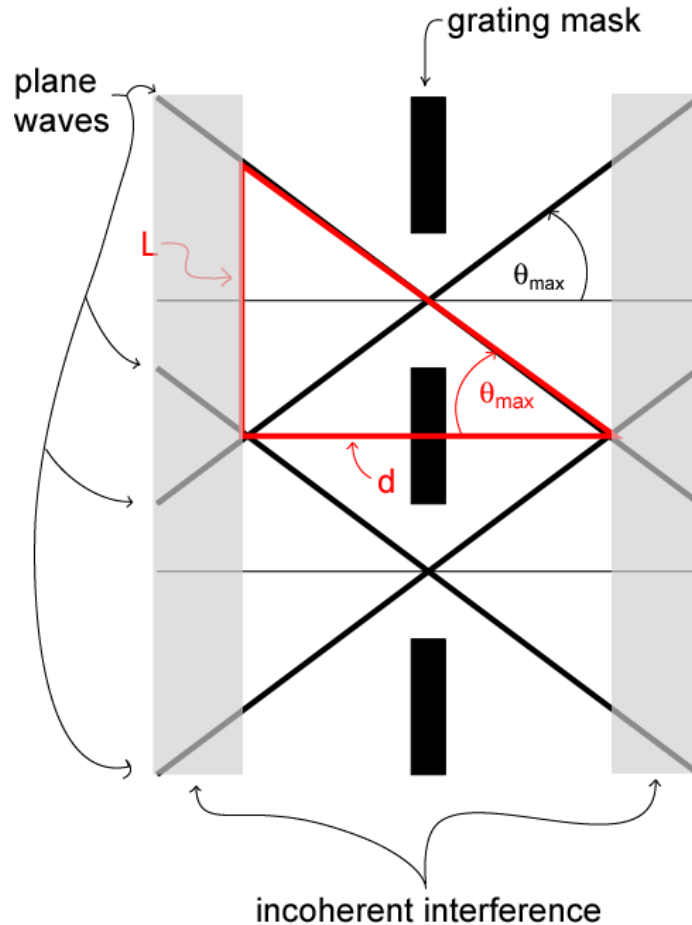
John Curtis

## Introduction

Optical sectioning can be done efficiently and relatively inexpensively using a grating image system. The system works by placing a mask grating in the field plane of a microscope's incoherent light source. This projects the mask into the focal plane of the specimen. The incoherence of the plane waves incident to and emitted from the masked light source causes random interference between plane waves leaving adjacent "slits" of the grating, which results in decreasing contrast as one moves (axially, forwards or backwards) away from the mask plane. For the microscope optics, the first (in terms of axial distance away from the mask plane) incoherent interference patterns are produced by plane waves incident to or emitted from adjacent slits at  $\pm$  half angles of acceptance for the objective lens. The half angle of acceptance, called  $\theta_{\max}$ , is defined by an objective's numerical aperture (NA),

$$NA = n_i \sin \theta_{\max}$$

The axial distance away from the mask plane where it's contrast is almost lost, called the defocus range, is approximately the point at which the  $\pm\theta_{\max}$  plane waves intersect. Accordingly the geometric formulation of the defocus range is as follows,



$$d = \frac{L}{\tan \theta_{\max}}$$

where  $d$  is the defocus range,  $L$  is the period of the grating mask, and  $\theta_{\max}$  is the half angle of objective acceptance. At axial distances  $\frac{d}{2}$  away from the mask plane incident and emergent plane waves (at  $\theta_{\max}$ ) begin to intersect and produce random or incoherent interference that decreases contrast. At axial distances greater than  $\frac{d}{2}$  away from the mask plane more plane waves (at incident and emergent angles smaller than  $\theta_{\max}$ ) intersect producing more incoherent interference that further decreases grating contrast. This causes the illuminance variance to be decreased at axial distances greater than  $\frac{d}{2}$  away from the grating in a way that is practically independent of the mask configuration. This allows one to modulate the objective's focal plane (with a depth of  $d$ ) without significantly influencing the unfocused portions of the image. Modulating the objective's focal plane by projecting the grating into it and then shifting the grating allows one to obtain a set of 3 images at different phase shifts that can be algebraically (digitally) combined in such a way that the (unmodulated) out of focus components of the resultant image is subtracted off and the focal plane, i.e. sectioned, image (with a depth  $d$ ) is recovered. Specifically one can obtain three images that are shifted by  $0^\circ$ ,  $90^\circ$  and  $180^\circ$ ,

$$img_0 = dc + \frac{img_{os}}{2}(1 + \sin(\theta + \phi_1)), \phi_1 = 0$$

$$img_{90} = dc + \frac{img_{os}}{2}(1 + \sin(\theta + \phi_2)), \phi_2 = \frac{\pi}{2}$$

$$img_{180} = dc + \frac{img_{os}}{2}(1 + \sin(\theta + \phi_3)), \phi_3 = \pi$$

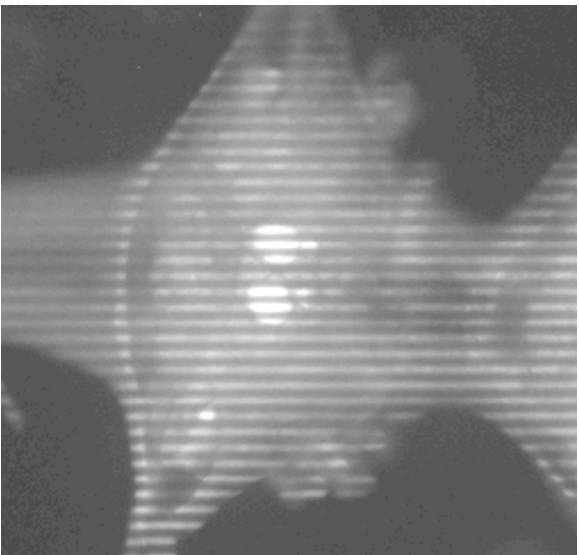
Combining the images to satisfy the trigonometric identity  $\sin^2x + \cos^2x = 1$ , gives,

$$img_{os} = \frac{1}{\sqrt{2}} \sqrt{(img_0 - img_{90})^2 + (img_{90} - img_{180})^2}$$

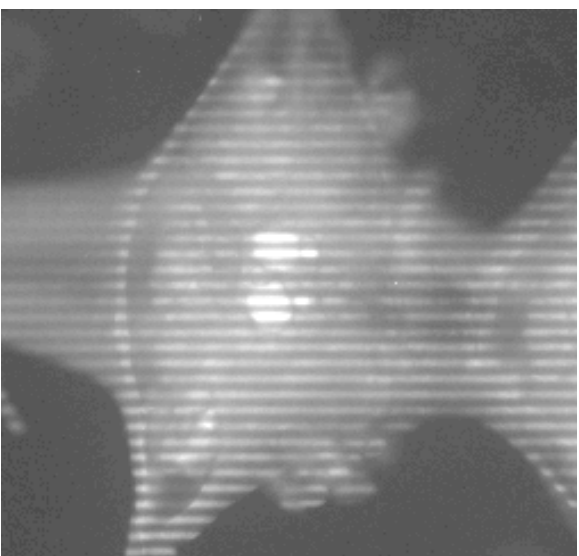
## Technical Considerations and Results

1. The camera/control unit combination "PXL2" has some hardware bug that intermittently causes it to not read in image data (giving error code: 168 C0\_EXP\_EXTRA\_DATA - finished data transfer, but extra data exists). The problems seem to arise when the camera's backplate temperature rises above 32 – 33 °C. Lowering the temperature setpoint would reduce the backplate temperature, but doing this seems to worsen the data transfer problem. The other camera "PXL1" works fine.
2. The Burleigh piezoelectric stage displays hysteresis that is more pronounced for larger voltage steps. Consequently, different voltages are needed for spatially equivalent up and down shifts. The piezoelectric operates over a range of 0 – 150 V and the National Instruments data acquisition board (nidaq) has an output voltage range of  $\pm 10$  V, so we set the Burleigh amplifier bias to 75 V and gain to 7.5. This was done so that a nidaq output of 10 V would give 150 V to the piezoelectric and  $-10$  V from the nidaq would give it 0 V. A 10 V step to the piezoelectric produces, roughly, a 1 pixel spatial shift. The period of the grating mask we used is approx. 14 pixels, so a typical quarter period shift ( $90^\circ$ ) took about a 35 V step. The precision of the piezoelectric is approx.  $\pm 0.01$  pixels.
3. The sectioned images show artifactual lines that are probably due to the harmonics produced by the square wave gratings. Figures 2 & 4 show average row (from bitmap matrices) power spectra for unsectioned (but modulated by the mask) and sectioned images. The unsectioned images have significant power at spatial frequencies of  $2k, 3k,$  and  $4k$ , where  $k = 0.0723$  is the gratings fundamental frequency. The power at these harmonic frequencies is amplified by the sectioning computation. The phase shifts between the images were found by calculating the average row cross-correlation between pairs of images. The shifts were accurate to within  $\pm 0.01$  pixels of the target quarter period, i.e.  $90^\circ$  shifts, e.g. with a period of  $\frac{1}{k}$  (calculated from the power spectra),  $90^\circ = \frac{1}{4k} = 3.4578$  pixels (see Figures 2 & 4). A filtering scheme needs to be developed that will eliminate the lines without compromising the image quality.

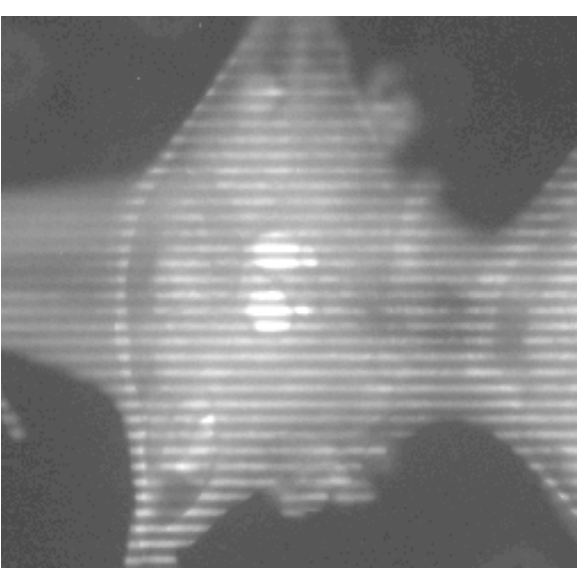
Figure 1. Comparison of sectioned and un-sectioned images of a leech ganglion



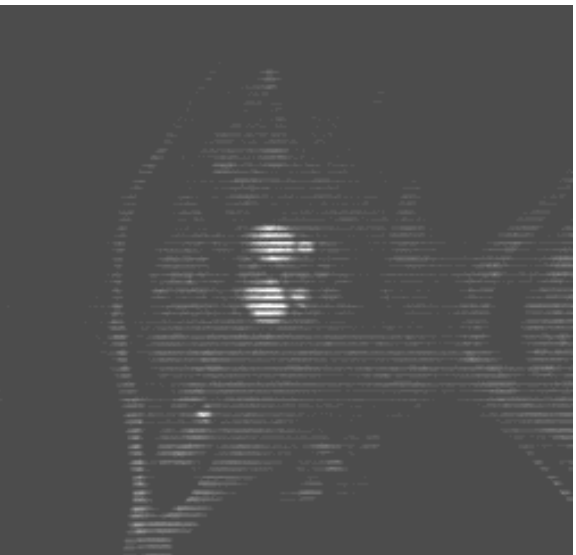
$img_0$



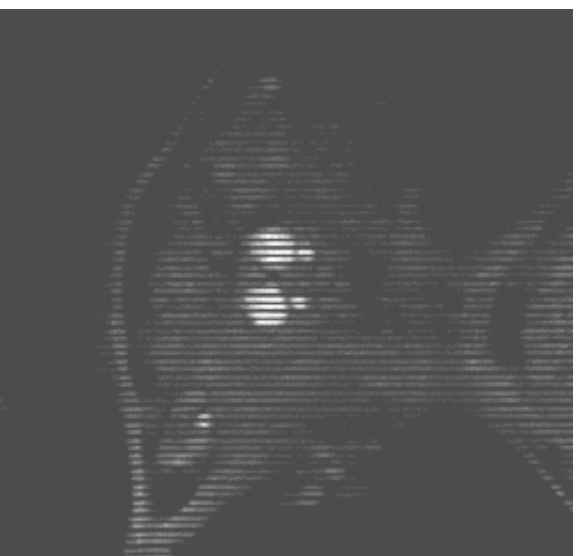
$img_{90}$



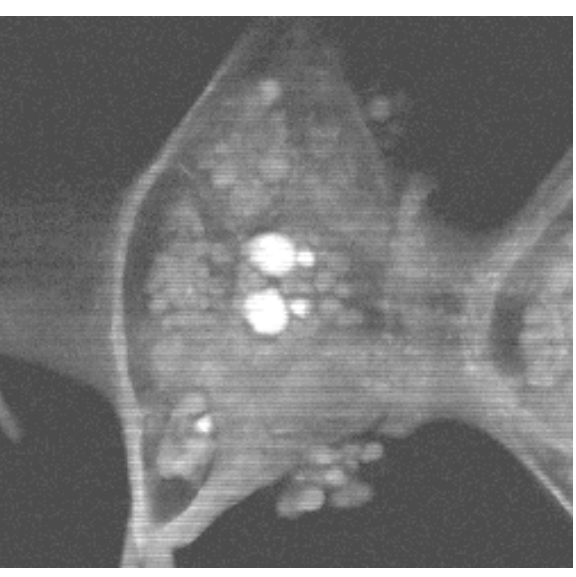
$img_{180}$



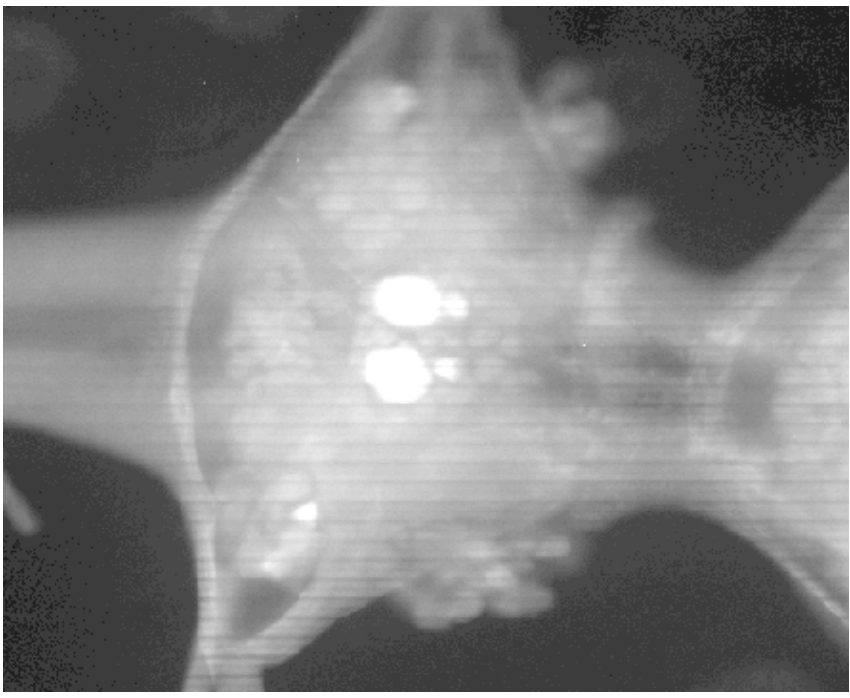
$(img_0 - img_{90})^2$



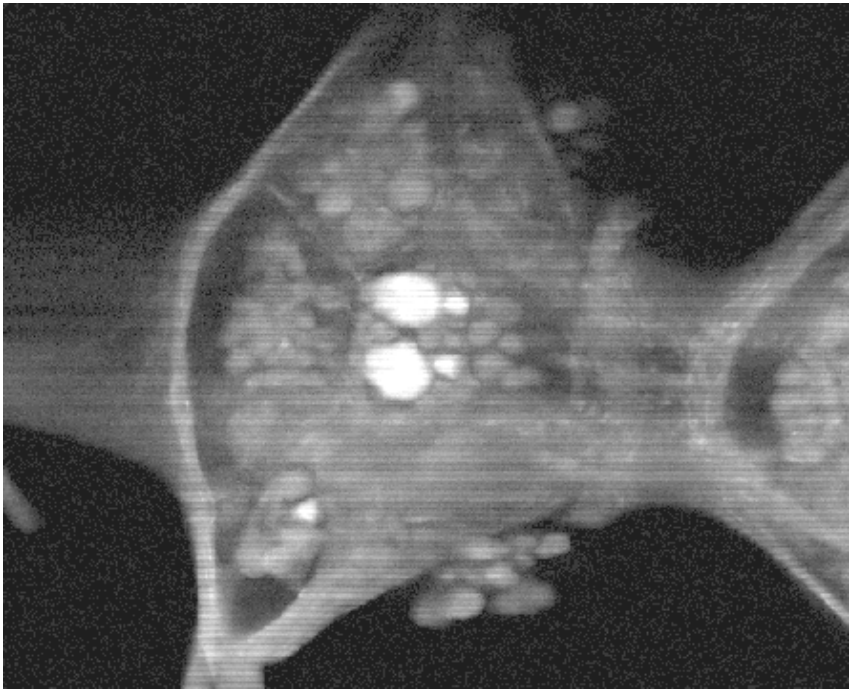
$(img_{90} - img_{180})^2$



$[(img_0 - img_{90})^2 + (img_{90} - img_{180})^2]^{1/2}$



Unsectioned Image:  $1/2(\text{img}_0 + \text{img}_{90})$



Sectioned Image:  $[(\text{img}_0 - \text{img}_{90})^2 + (\text{img}_{90} - \text{img}_{180})^2]^2$

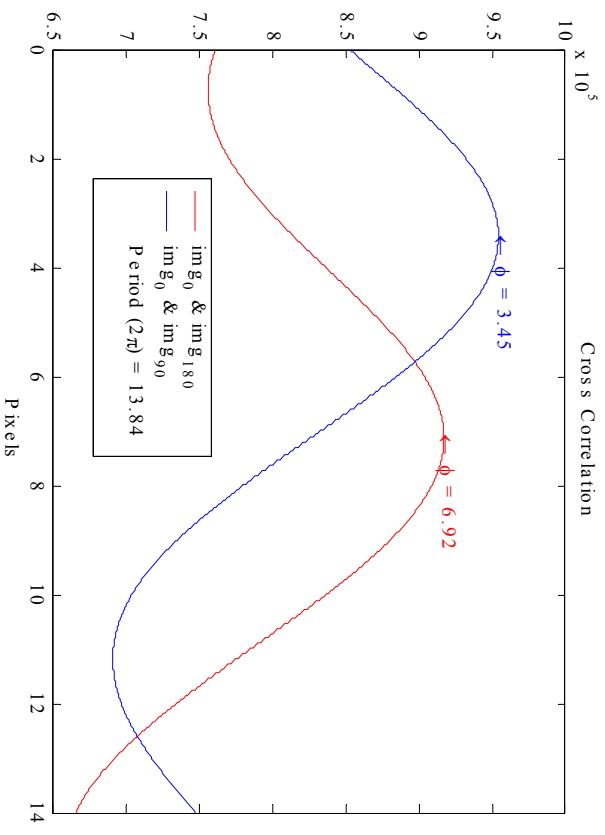
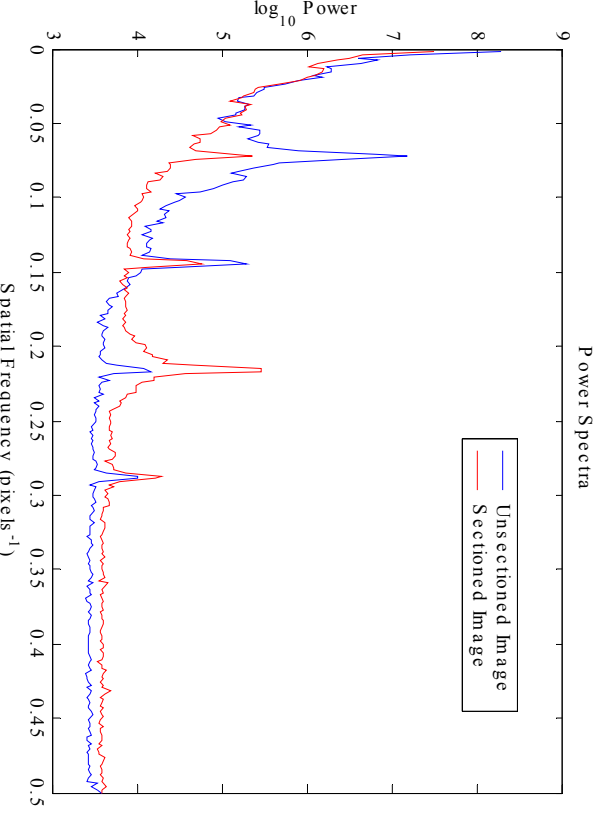
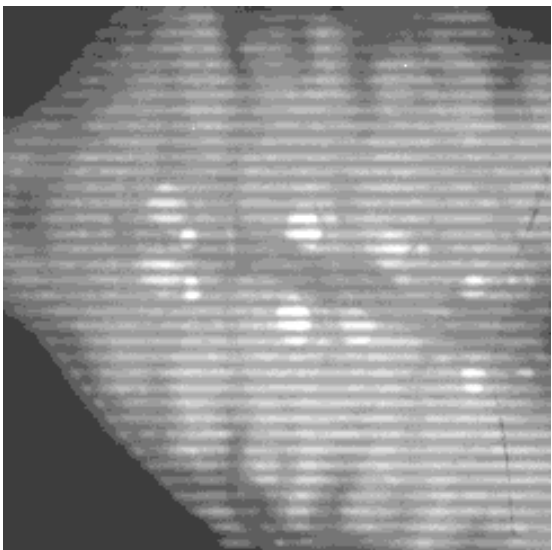
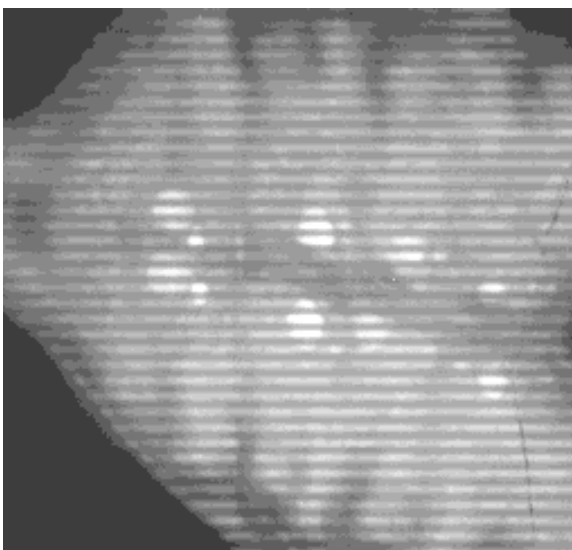


Figure 2. Comparison of sectioned and unsectioned image reconstructions. The power spectra (averaged over the bitmap rows of each image) reveals harmonics produced by the square wave grating. The cross correlation between the images (designated in the legend) show accurate 90 and 180 degree grating shifts. The artifactual lines in the images are most likely due to the square wave harmonics given the accuracy of the grating shifts.

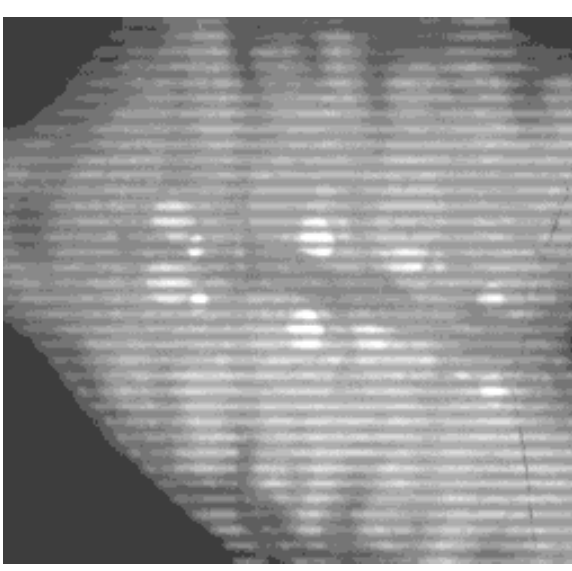
Figure 3. Comparison of sectioned, un-sectioned, and difference images of a leech ganglion



$img_0$



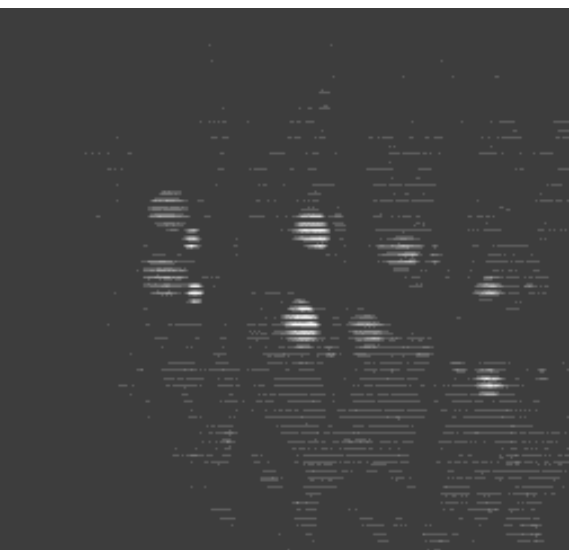
$img_{90}$



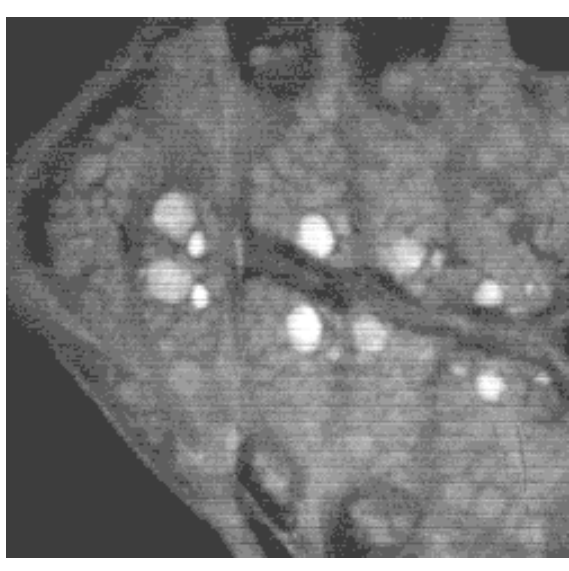
$img_{180}$



$(img_0 - img_{90})^2$



$(img_0 - img_{180})^2$



$[(img_0 - img_{90})^2 + (img_0 - img_{180})^2]^{1/2}$

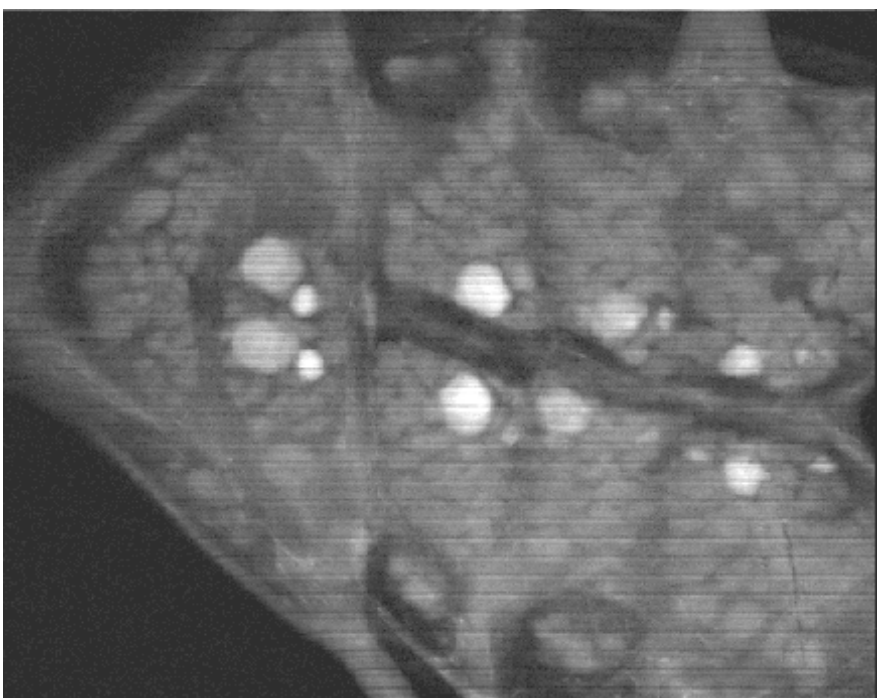
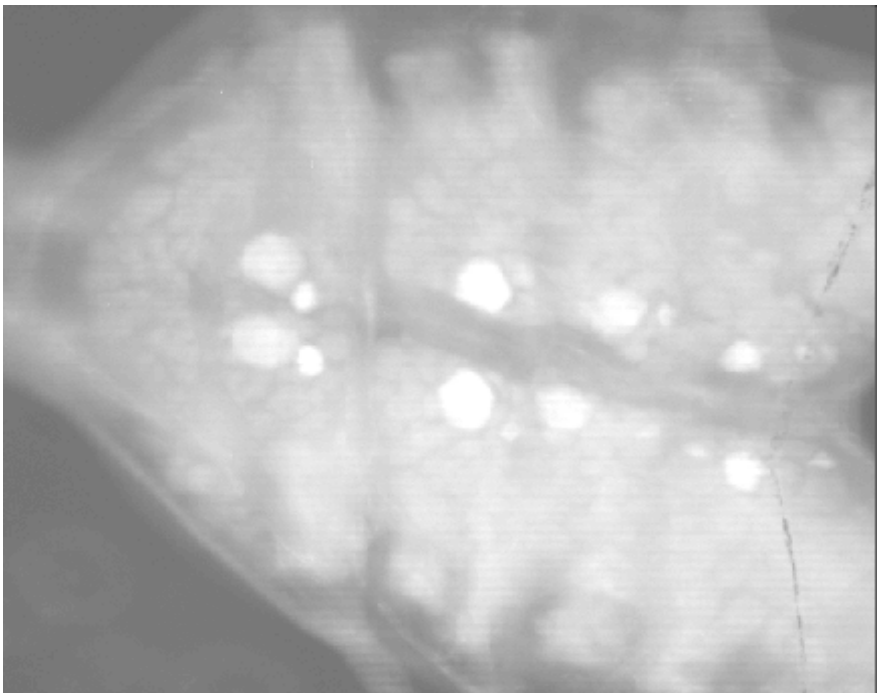


Figure 4. Comparison of reconstructed and unsectioned images. The power spectra for the sectioned image has less power at the grating frequency (approx  $0.07 \text{ pixels}^{-1}$ ) than the previous image, despite the fact that the 180 degree shifted image was a little short of a 180 degree shift (approx 171 degrees).

